



SPE 59316

Gel Propagation Through Fractures

R.S. Seright, SPE, New Mexico Petroleum Recovery Research Center

Copyright 2000, Society of Petroleum Engineers Inc.

This paper was prepared for presentation at the 2000 SPE/DOE Improved Oil Recovery Symposium held in Tulsa, Oklahoma, 3–5 April 2000.

This paper was selected for presentation by an SPE Program Committee following review of information contained in an abstract submitted by the author(s). Contents of the paper, as presented, have not been reviewed by the Society of Petroleum Engineers and are subject to correction by the author(s). The material, as presented, does not necessarily reflect any position of the Society of Petroleum Engineers, its officers, or members. Papers presented at SPE meetings are subject to publication review by Editorial Committees of the Society of Petroleum Engineers. Electronic reproduction, distribution, or storage of any part of this paper for commercial purposes without the written consent of the Society of Petroleum Engineers is prohibited. Permission to reproduce in print is restricted to an abstract of not more than 300 words; illustrations may not be copied. The abstract must contain conspicuous acknowledgment of where and by whom the paper was presented. Write Librarian, SPE, P.O. Box 833836, Richardson, TX 75083-3836, U.S.A., fax 01-972-952-9435.

Abstract

When gels are used for conformance control in reservoirs, a need exists to determine how much gel should be injected in a given application and where that gel is distributed (i.e., placed) in a naturally fractured reservoir. These parameters depend critically on the properties of gels in fractures. This paper describes an investigation of how Cr(III)-acetate-HPAM gels propagate and dehydrate (i.e., lose water through leakoff) during extrusion through fractures. These studies included fractures with lengths from 0.5 to 4 ft, and heights from 1.5 in. to 12 in., and gel injection fluxes from 129 to 33,100 ft/d.

Based on the experimental results, a model was developed to quantify gel propagation and dehydration during extrusion through fractures. The model indicated that to maximize gel penetration along fractures in field applications, the highest practical injection rate should be used.

Additional tests indicated that significant advantages could be realized for gels made using polymer with the highest available molecular weight. In addition to being potentially more cost-effective, these gels may penetrate deeper into a fracture system than gels made with lower molecular weight polymers.

Introduction

Gel treatments were often applied to improve conformance and reduce water or gas channeling in reservoirs.¹⁻⁵ During placement of conventional gel treatments, a fluid gelant solution typically flowed into a reservoir through porous rock and fractures. After the blocking agent was placed, chemical reactions (i.e., gelation) caused an immobile gel to form. In contrast, for the most successful treatments in naturally fractured reservoirs, the time required to inject large volumes (e.g., 10,000 to 37,000 bbls) of gel was typically greater than

the gelation time by a factor of 100.²⁻⁴ Thus, in these applications, formed gels extruded through fractures during most of the placement process.

A need exists to determine how much gel should be injected in a given application and where that gel distributes in a fractured reservoir. These parameters depend critically on the properties of gels in fractures. Therefore, we have a research program to determine these properties and to characterize gel placement in fractured systems.

Previous Experimental Work. Previous work demonstrated that gels do not flow through porous rock after gelation.⁶ This behavior is advantageous since the gel is confined to the fractures—it does not enter or damage the porous rock. Thus, after gel placement, water, oil, or gas can flow unimpeded through the porous rock, but flow through the fracture is reduced substantially.

However, extrusion of gels through fractures introduces new issues that are not of concern during placement of fluid gelant solutions. First, the pressure gradients required to extrude gels through fractures are greater than those for flow of gelants. For a Cr(III)-acetate-HPAM gel, the pressure gradient required for extrusion varied inversely with the square of fracture width (Fig. 1). In previous work,⁶⁻¹¹ we demonstrated that a minimum pressure gradient was required to extrude a given gel through a fracture. Once this minimum pressure gradient was exceeded, the pressure gradient during gel extrusion was insensitive to the flow rate. This behavior was attributed to a strong “slip” effect exhibited by the gel.^{6,8}

A second concern is that gels can concentrate (dehydrate) during extrusion through fractures.^{9,10} Depending on fracture width (see Fig. 2), this dehydration effect can significantly retard gel propagation (e.g., by factors up to 50). Figs. 1 and 2 apply to a one-day-old Cr(III)-acetate-HPAM gel at 41°C. This same gel was used for most of the experiments described in this paper. Specifically, our experiments used an aqueous gel that contained 0.5% Ciba Alcoflood 935 HPAM (molecular weight $\approx 5 \times 10^6$ daltons; degree of hydrolysis 5% to 10%), 0.0417% Cr(III) acetate, 1% NaCl, and 0.1% CaCl₂ at pH=6. All experiments were performed at 41°C (105°F). The gelant formulations were aged at 41°C for 24 hours (5 times the gelation time) before injection into a fractured core. We designate this gel as our standard Cr(III)-acetate-HPAM gel.

In earlier work,⁹ we showed that when large volumes of gel were extruded through a fracture, progressive plugging (i.e., continuously increasing pressure gradients) was not observed. Effluent from the fracture had the same appearance and a similar composition as those for the injected gel, even though a concentrated, immobile gel formed in the fracture. The concentrated gel formed when water leaked off from the gel along the length of the fracture. The driving force for gel dehydration (and water leakoff) was the pressure difference between the fracture and the adjacent porous rock. During gel extrusion through a fracture of a given width, the pressure gradients along the fracture and the dehydration factors were the same for fractures in 650-mD sandstone as in 50-mD sandstone and 1.5-mD limestone (Figs. 1 and 2).

Model 1. Previously,⁹ a simple model (Model 1) was developed that correctly matched the behavior during gel propagation and dehydration in a fracture with dimensions of 48x1.5x0.04 in. using an injection rate of 12.2 in.³/hr (200 cm³/hr). This model assumed the following:

- 1) Gel in the fracture existed in one of two forms: (a) flowing gel that had the same composition and properties as the originally injected gel, and (b) concentrated immobile gel. The flowing gel wormholed through the concentrated immobile gel.
- 2) The Darcy equation applied for water flow through gel, with a gel permeability to water, k_{gel} . The driving force for gel dehydration (and water leakoff) was the pressure difference between the fracture and the adjacent porous rock. The average distance that water traveled through the gel to reach the matrix was half the fracture width, $w_f/2$.
- 3) For a given length of fracture, the rate of water entering the fracture (in the form of gel) minus the rate of water leaving the fracture (again tied up as gel) equaled the rate of water leakoff through the fracture faces. (Water mass balance.)
- 4) No crosslinked polymer entered the porous rock. Any gel that concentrated (dehydrated) immediately became immobile. (Crosslinked polymer mass balance.)
- 5) At any point in the fracture, the gel permeability to water, k_{gel} , was related to the average gel composition by Eq. 1.

$$k_{gel}=0.00011+ 1.0 (C/C_o)^{-3} \dots\dots\dots (1)$$

In Eq. 1, k_{gel} had units of mD when the gel composition, C/C_o , was expressed relative to the composition of our standard Cr(III)-acetate-HPAM gel (i.e., 24-hr-old 0.5% Alcoflood 935 HPAM, 0.0417% Cr(III)-acetate). Originally, Eq. 1 was simply an empirical three-parameter fit that allowed the model to correctly quantify the rate of gel propagation through a 48x1.5x0.04-in. fracture. Since the original development of this model, we found independent support¹⁰ for two of the three parameters in Eq. 1 (i.e., the 1.0 mD coefficient and the -3 exponent for the concentration term). However, no quantitative basis was found for the third parameter, 0.00011 mD.

As a qualitative explanation for Eq. 1, we speculate that the concentration-dependent term accounted for progressive

dehydration of the concentrated immobile gel, while the constant term accounted for dehydration of flowing gel in the wormholes. At a given point in the fracture, the flowing gel was continually replenished, so it represented a source of gel with an unchanging concentration. Any flowing gel that dehydrated was added to the reservoir of concentrated gel. In contrast, the concentrated gel did not move and became ever more concentrated with time, so its average permeability to water continually decreased.

With an understanding of the mechanism for gel extrusion and dehydration in fractures, we ultimately hope to predict conditions, gel compositions, and gel volumes that provide the optimum gel placement in fractured reservoirs. To realize this goal, our model requires further testing. Therefore, in this paper, results are reported from extrusion experiments that used a range of fracture lengths and heights and a wide range of gel injection rates. An experiment was also performed using a gel prepared from a polymer with roughly twice the molecular weight of Alcoflood 935.

Effect of Injection Rate

Several experiments were performed to examine the effects of injection rate on gel extrusion and dehydration. Except for injection rate, these tests were identical to that described in Ref. 9. Specifically, in each test (at 41°C), we extruded 80 fracture volumes (226 in.³ or 3,700 cm³) of our standard 24-hr-old Cr(III)-acetate-HPAM gel through a 0.04-in.-wide fracture in a 4-ft-long, 650-mD Berea sandstone core. The cross-sectional area of the core was 2.25 in.² (1.5x1.5 in.), so the fracture height was 1.5 in. (3.8 cm). The total fracture volume was 2.84 in.³ (46.5 cm³), and the total pore volume of the system was about 25 in.³ (400 cm³). The core had five sections of equal length that were delineated by sets of fracture and matrix pressure taps. A fitting at the core outlet separated the effluent from the fracture and matrix. (Of course, a new core was used for each test.) To complement the 12.2 in.³/hr (200-cm³/hr) test that was described in Ref. 9, the three new tests were performed using gel injection rates of 30.5, 122, and 976 in.³/hr, respectively. Assuming that the total fracture volume was open to gel flow, the average velocities ranged from 413 to 33,100 ft/d for volumetric injection rates ranging from 12.2 to 976 in.³/hr (see Rows 2 and 3 of Table 1). For comparison, the velocity in a 100-ft-high, 0.04-in.-wide, two-wing fracture is 12,100 ft/d using an injection rate of 1 barrel per minute.

Table 1 summarizes the results from these tests. Consistent with our earlier findings,⁶⁻⁸ pressure gradients along the fracture were relatively insensitive to injection rate. The average pressure gradients (Row 4 of Table 1) ranged from 18 to 40 psi/ft for estimated gel velocities ranging from 413 to 33,100 ft/d. We suspect the pressure-gradient variations in Table 1 were caused by differences in the actual fracture width rather than by velocity differences.

Gel Front Propagation. The rate of gel front propagation increased significantly with increased injection rate (Row 5 of Table 1). For 413 ft/d, gel arrival at the end of a 4-ft-long fracture occurred after 15 fracture volumes of gel injection.

Only 1.7 fracture volumes of gel were required when the velocity was 33,100 ft/d. Evidently, the gel had less time to dehydrate as the injection rate increased. With a lower level of gel dehydration (concentration), the gel propagated a greater distance for a given total volume of gel injection. This result has important consequences for field applications. It suggests that gels should be injected at the highest practical rate in order to maximize penetration into the fracture system.

During gel injection, pressures along the fracture indicated the rate of propagation of the gel front. For three of the experiments (413 ft/d, 1,030 and 4,130 ft/d, respectively), Fig. 3 shows the volume of gel required to reach a given distance along a 4-ft-long fracture. The solid symbols show the actual data points, while the open circles with the dashed lines show predictions from our model (Model 1). As mentioned earlier, the three-parameters in Eq. 1 were originally fitted to describe the 413-ft/d experimental results. Thus, the match between the experiment and the predictions were expected for this case. However, for the other two velocities, the model predictions were typically 50% to 70% greater than the actual values. This finding indicates that our model needs refinement.

Gel Dehydration. For each experiment, a special outlet fitting segregated the effluent from the fracture and that from the porous rock. Fig. 4 plots the fraction of the effluent that was produced from the porous rock. Rows 6 and 7 of Table 1 summarize these results. In each case, the peak in flow from the porous rock was observed when gel arrived at the end of the fracture. Expressed as a fraction of the total flow, the magnitude of this peak decreased with increased injection rate—from 100% at 413 ft/d to 39% at 33,100 ft/d (Row 6 of Table 1). After gel breakthrough, the fraction of flow from the porous rock decreased in an exponential fashion. After 75-80 fracture volumes of gel injection, this fraction varied from 35% at 413 ft/d to 5% at 33,100 ft/d (Row 7 of Table 1). Of course, at any given time, the fraction of flow from the fracture plus that from the porous rock summed to unity. As a reminder, the total injection rate was constant during a given experiment.

The chromium and HPAM concentrations were determined for the effluent from both the fracture and the porous rock. In all cases, no significant chromium or HPAM were produced from the porous rock. Thus, only water (brine) flowed through the porous rock. Of course, the source of this flow was water that left the gel in the fracture—i.e., water from the gel dehydration process. Our findings confirm that crosslinked polymer (gel) does not enter or flow through porous rock.

Before gel arrival at the end of the fracture, virtually all fluid was produced from the fracture, and this fluid consisted of brine with no chromium or HPAM. This result was expected. Before gel injection, the calculated flow capacity of the fracture was 3,400 times greater than the flow capacity of the porous rock. After gel breakthrough, the composition and physical appearance of gel produced from the fracture were very similar to those of the injected gel. Details of these analyses can be found in Ref. 10.

After 80 fracture volumes of gel injection, the fracture was opened to reveal a rubbery gel that completely filled the

fracture. These gels were analyzed for chromium and HPAM as a function of length along the fracture. (Details can be found in Ref. 10.) Row 8 of Table 1 reports the average factor by which gel in the fracture was concentrated for each experiment. Expressed relative to the concentration of the injected gel (C/C_o), gel was concentrated by an average factor of 27 at 413 ft/d and by 4 at 33,100 ft/d. Of course, since fixed volumes of gel were injected, the duration of gel injection varied inversely with injection rate. Since gel in the fracture was under pressure for a shorter time in the faster experiments, the gel had less time to dehydrate. Consequently, the degree of dehydration decreased with increased injection rate. These results further support our conclusion that in field applications, gels should be injected at the highest practical rate to maximize penetration into the fracture system.

Effect of Fracture Height

To this point, our fracture heights were 1.5 in. (3.8 cm). Will gel extrusion and dehydration be affected by fracture height? To address this question, two experiments were performed with fracture heights of 12 in. Fig. 5 illustrates the fractured cores that were used. The cores were formed by stacking two 12×12×3-in. 650-mD Berea sandstone slabs. Spacers were used to separate the two slabs by 0.04 in. (0.1 cm) to form a 12×12×0.04-in. fracture. Because of the method of construction, the faces of the fracture were fairly smooth. (In contrast, the fractures described in the previous section were formed by cracking the core open using a special method that was described earlier.⁶ In our experience, the roughness of the fracture surfaces did not affect the performance during gel extrusion.) The total fracture volume was 5.67 in.³ (92.9 cm³) and the total pore volume of the system was 173 in.³ (2,831 cm³). The fractures were actually oriented horizontally, but for consistency, we identify the fracture “height” as the dimension perpendicular to the fracture length and width dimensions. A manifold distributed the injected gel evenly over the 12-in. height of the fracture. A similar manifold collected the effluent from the fracture. Two production ports also allowed collection of effluent from each of the matrix slabs.

In the first experiment, 30 fracture volumes (~170 in.³ or 2,800 cm³) of our standard 24-hr-old Cr(III)-acetate-HPAM gel were injected at a fixed rate of 30.5 in.³/hr (500 cm³/hr). Considering the cross-sectional flow area of the fracture (12×0.04 in.), the injection flux or velocity was 129 ft/d (164 cm/hr). This value compares with a flux of 1,030 ft/d when injecting gel at a rate of 30.5 in.³/hr into our earlier 48×1.5×0.04-in. fractured cores.

In the second experiment, 61 fracture volumes (~350 in.³ or 5,700 cm³) of gel were injected at a fixed rate of 98 in.³/hr (1,600 cm³/hr). The injection flux in this experiment was 413 ft/d. For both experiments, the pressure gradient during gel injection averaged 29 psi/ft. This value was very similar to those observed earlier during extrusion through fractures of the same width, but with heights of 1.5 in. (Table 1).

Consistent with our earlier results, no significant HPAM or chromium was produced from the matrix during these

experiments. For the 129- and 413-ft/d experiments, gel breakthrough was noted after injecting 6 and 2.6 fracture volumes of gel, respectively. After gel breakthrough, the gel produced from the fractures was similar in composition to that for the injected gel. No significant fluid was produced from the matrix until gel breakthrough. At gel breakthrough, the fraction of fluid from the matrix jumped to 97% of the total flow for the 129-ft/d experiment and to 91% of the total flow for the 413-ft/d experiment (Fig. 6). With further gel injection in the 129-ft/d experiment, this fraction gradually declined to 55% of the total after injection of 30 fracture volumes. During the 413-ft/d experiment, the matrix fractional flow declined to 33% after 30 fracture volumes and 17% after 61 fracture volumes. (The data jumps in Fig. 6 occurred when switching injection pumps.)

Wormholes. For both experiments, near the end of gel injection, dyed gel of the same composition was injected. For the 129- and 413-ft/d experiments, dye breakthrough was noted after injecting 0.55 in.³ (0.097 fracture volumes) and 0.49 in.³ (0.086 fracture volumes), respectively. At the time of dyed-gel breakthrough, the average gel dehydration factors for newly injected gel were 55% and 17%, respectively (because these were the fractions of total flow produced as water from the end of the matrix). Thus, the estimated volumes of the pathways for the dyed gel were 0.25 in.³ [i.e., 0.55x(1-0.55)] or 0.044 fracture volumes for the 129-ft/d experiment and 0.4 in.³ [i.e., 0.49x(1-0.17)] or 0.071 fracture volumes for the 413-ft/d experiment. These results suggest that the injected gel formed small-volume wormholes through concentrated gel.

Consistent with this suggestion, wormhole pathways were noted (highlighted by the dye) through the concentrated gel in the fracture after opening the fracture at the end of the experiments. Typically, these wormholes were 0.1 to 0.2 in. in height, compared to the total fracture height of 12 in. In the 129-ft/d experiment, one wormhole in the center of the pattern appeared dominant, while six other significant wormholes were present in various locations. A limited amount of branching was noted on these wormholes. In contrast, for the 413-ft/d experiment, highly branched wormhole patterns were found after dye injection. For both experiments, after removing the gel from the fractures, streaks of dyed rock were noted under the wormholes—revealing the leakoff pathways for water that dehydrated from the gel.

Dyed-gels were also injected near the end of the 1,030-ft/d and 4,130-ft/d experiments in the 48x1.5x0.04-in. fractures. Results indicated that the wormhole volumes were 0.10 and 0.14 fracture volumes, respectively. Since the wormhole volumes were 4% to 14% of the fracture volume, actual velocities for the flowing gel in the wormholes were 7 to 22 times faster than indicated by our flux values (i.e., calculated assuming that the entire fracture cross-section was open to flow).

Model 2

In view of the deficiencies of our first model, a second model was developed to account for our new results. Model 2 was inspired by a re-plot of the data in Figs. 4 and 6. Specifically,

Fig. 7 plots the average leakoff rate (u_i , in ft³/ft²/d or ft/d) versus time (t , in days) for the six experiments. Results are also included from a seventh experiment where the gel was forced through a 6x1.5x0.04-in. fracture at an average flux of 413 ft/d. (Details of this experiment can be found in Ref. 11.) At any given time, the average leakoff rate was simply the total flow rate from the matrix (at the end of the core) divided by the total fracture area in the core. For a given experiment, Fig. 7 included only the data after the peak in flow from the porous rock. Eq. 2 provided an excellent fit of the data.

$$u_i = 0.05 t^{-0.55} \dots\dots\dots (2)$$

Eq. 2 provides leakoff rates that are averaged over the length of the fracture (more specifically, over the gel-contacted length of the fracture). Eq. 3 relates the average leakoff rate to the local leakoff rate, u_i , at a given distance, L , along the fracture.

$$u_i = \int u_i dL \dots\dots\dots (3)$$

The rate of gel front propagation, dL/dt , in a 0.04-in.-wide fracture can be found from a mass balance (Eq. 4).

$$h_f w_f dL/dt = q_i - 2 h_f L u_i \dots\dots\dots (4)$$

In Eq. 4, h_f is fracture height, w_f is fracture width, and q_i is total volumetric injection rate. Combined with Eq. 2, Eq. 4 can easily be applied to predict rates of gel front propagation and gel dehydration. These equations form the basis for Model 2. In Fig. 8, the open symbols with the dashed lines show gel front positions predicted for three injection rates in 48x1.5x0.04-in. fractures. The solid symbols show the experimental values. A comparison of Figs. 3 and 8 reveals that except for the 413-ft/d case, the experimental data were matched better by Model 2 than by Model 1. Of course, Model 2 provides an excellent match for the experimental leakoff rates (Fig. 7).

Additional comparisons of experimental results and predictions from Models 1 and 2 are included in Table 2. This table lists results from experiments in the 12x12x0.04-in. fractures as well as those in the 48x1.5x0.04-in. fractures. Regarding the rate of gel propagation, Model 2 gave more accurate predictions than Model 1 when rates were high. The success of Model 1 at 413 ft/d was not surprising since this model was based on a curve fit of low-rate data. Nevertheless, Model 2 provided reasonable predictions at low rates.

Regarding leakoff data (i.e., flow from the matrix), Model 2 generally provided significantly better predictions than Model 1, although Model 1 performed acceptably at low rates in the 4-ft-long fractures. Model 1 consistently out-performed Model 2 in predicting the final average gel composition in the fractures. Except at the highest rate, concentration predictions from Model 2 were typically 60% to 90% too high. However, some experimental error was associated with our concentration

determinations. Also, evidence exists that some free chromium and uncrosslinked HPAM leaked off into the porous rock during gel dehydration.¹¹ Furthermore, the flowing gel may be slightly more concentrated than the originally injected gel.^{10,11} These phenomena could decrease the mass of gel that accumulated at a given point in the fracture—thus, mitigating the concentration over-predictions for Model 2.

Predictions in Long Fractures

A key motivation for this work is a need to quantify how gels propagate through fractures in field applications. Of course, these fractures are much longer and higher than those examined experimentally in this study. To accurately predict behavior in field applications, a satisfactory model is required for gel propagation and dehydration during extrusion.

Model 2. Further testing is needed to establish whether we have the correct model. If forced to choose the best model at this point, Model 2 would be selected. This model can easily be applied to make predictions for field applications. Fig. 9 presents these predictions for three injection rates (0.1 to 10 barrels per minute, BPM) in 0.04-in.-wide, two-wing fractures using our standard Cr(III)-acetate-HPAM gel. At a given rate, Fig. 9 shows the gel volume that must be injected to achieve a given distance of penetration along the fracture. This volume increased with distance of penetration raised approximately to the 1.5 power. For a given distance of penetration, the required gel volume decreased substantially with increased injection rate. For example, to penetrate 200 ft, the required gel volume was 5 times less at 10 BPM than at 1 BPM. Therefore, to maximize gel penetration, the highest practical injection rate should be used.

Since Model 2 was based strictly on data in 0.04-in.-wide fractures, we only have confidence in predictions for fractures of that width. Work is underway to determine relations like Eq. 2 for other fracture widths. These relations will be used to predict gel placement in fractured systems.¹²

Model 1. Gel propagation rates were also predicted using Model 1. These predictions were documented in Ref. 10. This model suggested that the maximum distance of gel penetration into a fracture is inversely proportional to the square root of gel permeability and directly proportional to the 1.5 power of fracture width. Model 1 also predicted that the maximum distance of gel penetration is proportional to the square root of injection rate. Consistent with Model 2, Model 1 indicated that to maximize gel penetration along a fracture, the highest practical injection rate should be used. However, Model 1 was generally much more pessimistic than Model 2 concerning the distance that gel can propagate into a fracture. This result occurred because Model 1 allowed greater leakoff rates than Model 2 at intermediate and long times. Since we believe that Model 2 more correctly accounts for leakoff (Fig. 7), we currently have more confidence in Model 2.

Effect of Polymer Molecular Weight

In the work discussed to this point, the only polymer used was Alcoflood 935 HPAM. The manufacturer (Ciba) stated that this polyacrylamide had a molecular weight between 7 and 9×10^6 daltons and a 10% degree hydrolysis. For comparison, Marathon determined that this polymer had a molecular weight of 5×10^6 daltons and a degree of hydrolysis between 5% and 10% (personal communication with R.D. Sydansk).

We wondered whether a gel made with a higher molecular weight polymer could be more cost-effective and/or exhibit more desirable extrusion properties in fractures. To answer this question, we studied a second HPAM polymer, Ciba Percol 338, which Ciba stated had a molecular weight between 12 and 14×10^6 daltons and a 10% degree of hydrolysis. A range of formulations was prepared to identify a gel composition that provided behavior similar to that for a gel with 0.5% Alcoflood 935 and 0.0417% Cr(III)-acetate. In all formulations, the ratio of HPAM to Cr(III)-acetate was fixed (at 12:1), the brine used for gelant preparation contained 1% NaCl and 0.1% CaCl₂, and the gel was aged for 24 hours at 41°C. Similarity of behavior was judged by tonguing from a bottle. The most similar gel contained 0.2% Percol 338 HPAM and 0.0167% Cr(III)-acetate. This composition was used during extrusion tests. In the remainder of this paper, the Alcoflood 935 gel will be called the “low-Mw gel,” while the Percol 338 gel will be called the “high-Mw gel.”

The selected high-Mw gel (0.2% HPAM, 0.0167% Cr(III)-acetate, 1% NaCl, 0.1% CaCl₂ aged for 24 hours at 41°C) was forced through a 4-ft-long fractured Berea sandstone core. The average fracture width was 0.04 in. (0.1 cm), and 39 fracture volumes of gel were injected at a fixed rate of 24.4 in.³/hr.

Gel Propagation. Near the end of gel injection, the pressure gradient in the fracture averaged 4.1 psi/ft. This value was about seven times lower than the average pressure gradients observed during injection of the low-Mw gel (with 0.5% HPAM) into a similar fractured core. This result suggests that gels made from polymers with higher molecular weights may be more likely to extrude deep into a fracture system without exceeding wellbore pressure constraints.

Consistent with our earlier observations, no significant chromium or HPAM was produced from the porous rock during this experiment. (Details can be found in Ref. 10.) For effluent from the fracture, chromium and HPAM were first detected after injecting 4 fracture volumes of gel. However, the chromium and HPAM concentrations did not approach the injected concentration until about 13 fracture volumes of gel. Thus, some ambiguity exists about the time at which gel arrived at the end of the fracture. After 13 fracture volumes of gel injection, the chromium and HPAM concentrations in the effluent were similar to those for the injected gel.

Gel Dehydration. At the core outlet, the fraction of the fluid produced from the fracture versus from the matrix is shown in Fig. 10. This figure reveals that no significant fluid was produced from the matrix until after 13 fracture volumes of gel

were injected. By analogy with the analysis associated with Figs. 4 and 6, Fig. 10 suggests that gel breakthrough occurred at 13 fracture volumes rather than at 4 fracture volumes. The fraction of flow in the matrix in Fig. 10 peaked at 78% of the total. Near the end of gel injection, 59% of the flow was produced from the fracture, while 41% was produced from the porous rock. Fig. 11 plots the matrix effluent data from Fig. 10 in the same manner as shown in Fig. 7. The solid line in Fig. 10 shows the curve fit for the low-Mw gels from Fig. 7. The similarity of leakoff for low-Mw and high-Mw gels indicates that the two gels dehydrate and propagate in similar ways.

At the end of the experiment, the fracture was opened, and the gel in the fracture was analyzed. The chromium and HPAM concentrations for gel in the fracture were 10 to 20 times higher than the values in the original gel. For comparison, in previous experiments with the low-Mw gel, the gel in the fracture after injecting ~40 fracture volumes was also from 10 to 20 times more concentrated than the injected gel. This similarity in degree of concentration for the low-Mw and high-Mw gels also suggests that the two gels dehydrate at roughly the same rate.

As mentioned previously, the pressure gradient needed to extrude the high-Mw gel through the fracture was about seven times lower than that for low-Mw gel. Thus, gels made from polymers with higher molecular weights may be more likely to extrude deep into a fracture system without exceeding wellbore pressure constraints. Since the high-Mw gel required 2.5 times less polymer and chromium than the low-Mw gel, a significant economic advantage may be realized by preparing gels with polymers having the highest available molecular weight.

Conclusions

The following conclusions apply to 1-day-old Cr(III)-acetate-HPAM gels at 41°C:

1. In 0.04-in-wide fractures with lengths from 0.5 to 4 ft, heights from 1.5 in. to 12 in., and for injection fluxes from 129 to 33,100 ft/d, the average rate of gel dehydration and leakoff (u_i , in ft/d or ft³/ft²/d) was described well using: $u_i = 0.05 t^{0.55}$, where t is time in days.
2. The above equation formed the basis of a model that effectively accounted for gel propagation and dehydration during extrusion through 0.04-in-wide fractures.
3. The model and experimental data indicate that to maximize gel penetration along fractures in field applications, the highest practical injection rate should be used.
4. Significant advantages may be realized for gels prepared using polymer with the highest available molecular weight. In addition to being potentially more cost-effective, these gels may penetrate deeper into a fracture system than gels made with lower molecular weight polymers.

Nomenclature

- C = produced concentration, g/m³
 C_o = injected concentration, g/m³
 h_f = fracture height, ft [m]
 k_f = fracture permeability, darcys [μm^2]

k_{gel} = gel permeability to water, darcys [μm^2]

L = distance along a fracture, ft [m]

L_f = fracture length, ft [m]

Dp = pressure drop, psi [Pa]

dp/dl = pressure gradient, psi/ft [Pa/m]

q_i = total injection rate, BPD [m³/d]

u_i = local water leakoff rate, ft/d [cm/s]

u_l = water leakoff rate, ft/d [cm/s]

t = time, s

w_f = fracture width, in. [m]

Acknowledgments

Financial support for this work is gratefully acknowledged from the National Petroleum Technology Office of the United States Department of Energy, BP-Amoco, Chevron, China National Petroleum Corp., Chinese Petroleum Corp., Halliburton, Marathon, Saga, Schlumberger-Dowell, Shell, and Texaco. I thank Richard Schrader and Kate Wavrik for performing the experiments.

References

1. Seright, R.S. and Liang, J.: "A Survey of Field Applications of Gel Treatments for Water Shutoff," paper SPE 26991 presented at the 1994 SPE III Latin American & Caribbean Petroleum Engineering Conference, Buenos Aires, Argentina, April 27-29.
2. Sydansk, R.D. and Moore, P.E.: "Gel Conformance Treatments Increase Oil Production in Wyoming," *Oil & Gas J.* (Jan. 20, 1992) 40-45.
3. Borling, D.C.: "Injection Conformance Control Case Histories Using Gels at the Wertz Field CO₂ Tertiary Flood in Wyoming, USA," paper SPE 27825 presented at the 1994 SPE/DOE Symposium on Improved Oil Recovery, April 17-20.
4. Hild, G.P. and Wackowski, R.K.: "Reservoir Polymer Gel Treatments To Improve Miscible CO₂ Flood," *SPEE* (April, 1999) 196-204.
5. Lane, R.H. and Sanders, G.S.: "Water Shutoff Through Fullbore Placement of Polymer Gel in Faulted and in Hydraulically Fractured Producers of the Prudhoe Bay Field," paper SPE 29475 presented at the 1995 SPE Production Operations Symposium, Oklahoma City, April 2-4.
6. Seright, R.S.: "Gel Placement in Fractured Systems," *SPEPF* (Nov. 1995), 241-248.
7. Seright, R.S.: "Use of Preformed Gels for Conformance Control in Fractured Systems," *SPEPF* (Feb. 1997) 59-65.
8. Seright, R.S.: "Gel Dehydration During Extrusion Through Fractures," *SPEPF* (May 1999) 110-116.
9. Seright, R.S.: "Mechanism for Gel Propagation Through Fractures," paper SPE 55628 presented at the 1999 SPE Rocky Mountain Regional Meeting, Gillette, May 15-19.
10. Seright, R.S.: "Using Chemicals to Optimize Conformance Control in Fractured Reservoirs," Annual Technical Progress Report (U.S. DOE Report DOE/BC/15110-2), U.S. DOE Contract DE-AC26-98BC15110, (Sept. 1999) 3-52.
11. Seright, R.S.: "Improved Methods for Water Shutoff," Final Technical Progress Report (U.S. DOE Report DOE/PC/91008-14), U.S. DOE Contract DE-AC22-94PC91008, BDM-Oklahoma Subcontract G4S60330 (Oct. 1998) 21-54.
12. Seright, R.S. and Lee, R.L.: "Gel Treatments for Reducing Channeling Through Naturally Fractured Reservoirs," *SPEPF* (Nov. 1999) 269-276.

SI Metric Conversion Factors

cp x 1.0*	E-03	= Pa·s
ft x 3.048*	E-01	= m
in. x 2.54*	E+00	= cm
mD x 9.869 233	E-04	= μm^2
psi x 6.894 757	E+00	= kPa

*Conversion is exact.

Table 1—Effect of injection rate on gel propagation during injection of 80 fracture volumes of gel.

1	Fracture dimensions (L_f \times h_f \times w_f)	48 \times 1.5 \times 0.04-in.			
2	Injection rate, in. ³ /hr	12.2	30.5	122	976
3	Estimated velocity in the fracture, ft/d	413	1,030	4,130	33,100
4	Average pressure gradient, psi/ft	28	29	40	18
5	Gel front arrival at core end, fracture volumes	15	6.0	4.0	1.7
6	Peak fraction of matrix flow, %	100	93	75	39
7	Final fraction of flow produced from matrix, %	35	26	16	5
8	Average C/C_o in fracture at end of experiment	27	17	11	4

Table 2—Measurements versus predictions: Model 1 [$k_{gel}=0.00011+1.0(C/C_o)^{-3}$] and Model 2 [$u_l = 0.05 f^{0.55}$].

Fracture dimensions (L_f \times h_f \times w_f)	48 \times 1.5 \times 0.04-in.				12 \times 12 \times 0.04-in.	
Injection rate, in. ³ /hr	12.2	30.5	122	976	30.5	98
Estimated velocity in the fracture, ft/d	413	1,030	4,130	33,100	129	413
Total fracture volumes of gel injected	80	80	80	80	30	61
Gel arrival at core end, fracture volumes						
Actual	15	6.0	4.0	1.7	6.0	2.6
Predicted by Model 1	14.3	9.9	6.0	3.0	7.7	5.2
Predicted by Model 2	12.3	6.4	2.8	1.5	10.4	4.7
Peak fraction of matrix flow, %						
Actual	100	93	75	39	97	91
Predicted by Model 1	96	94	90	80	92	88
Predicted by Model 2	95	91	76	42	95	87
Fraction of flow produced from end of matrix, %						
Actual	35	26	16	5	55	17
Predicted by Model 1	35	13	6	3	16	6
Predicted by Model 2	34	23	12	5	53	21
Average C/C_o in fracture at end of experiment						
Actual	27	17	11	4	12	14
Predicted by Model 1	31	21	14	8	12	11
Predicted by Model 2	44	32	19	8	22	23

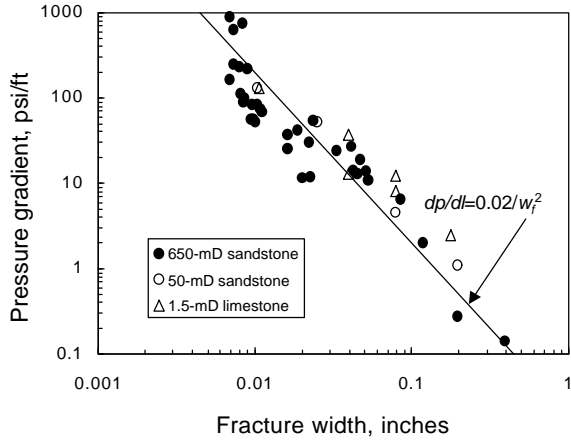


Fig. 1—Pressure gradients required to extrude a gel through open fractures (from Ref. 9).

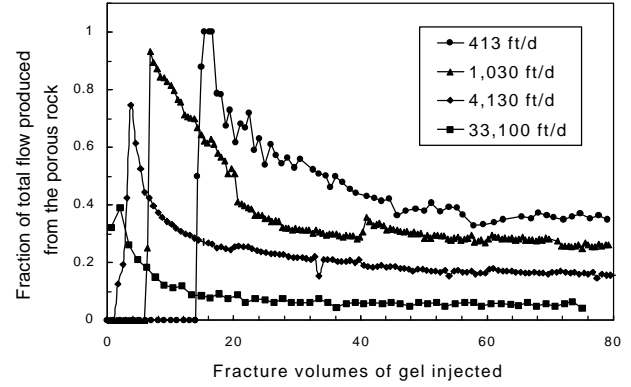


Fig. 4—Fraction of flow produced from the porous rock during gel injection into 48x1.5x0.04-in. fractures at various rates.

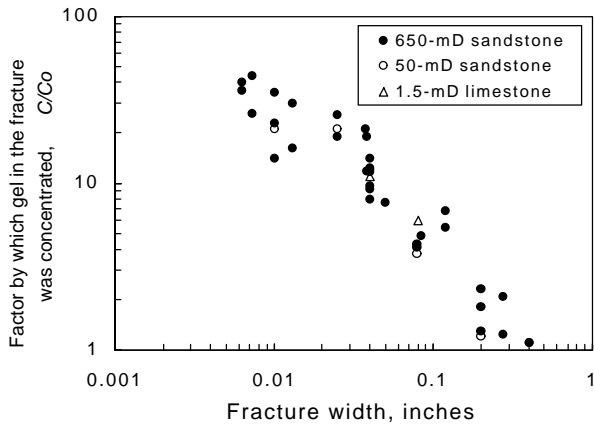


Fig. 2—Degree of gel dehydration versus fracture width (from Ref. 9).

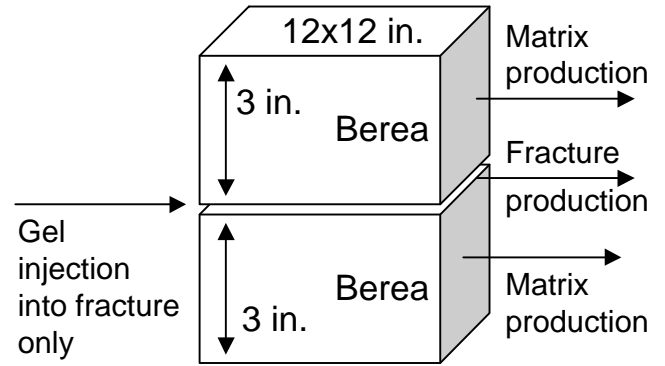


Fig. 5—Schematic of experiment in 12x12x0.04-in. fracture.

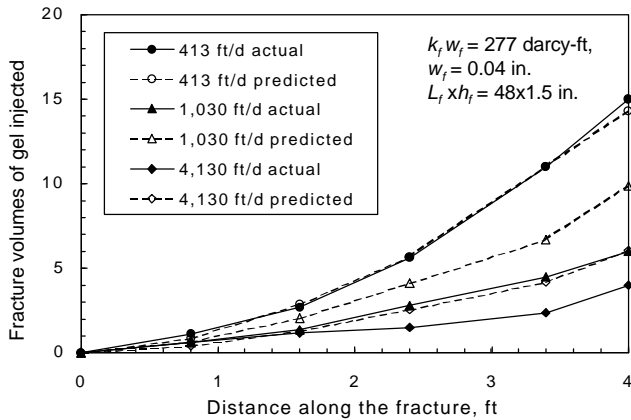


Fig. 3—Gel propagation in 48x1.5x0.04-in. fractures. Model 1: $k_{ge} = 0.00011 + 1.0(C/C_0)^3$.

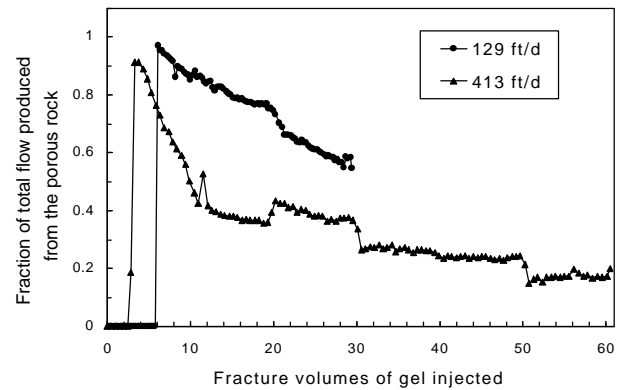


Fig. 6—Fraction of flow produced from the porous rock during gel injection into 12x12x0.04-in. fractures at two rates.

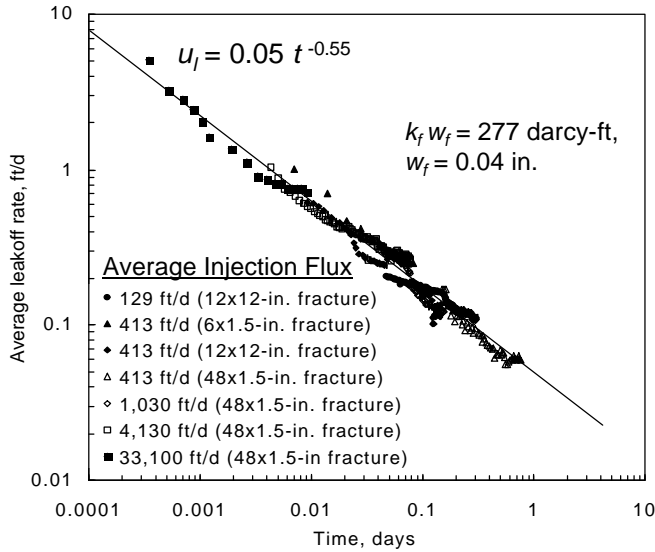


Fig. 7—Average leakoff rate from seven experiments at different velocities.

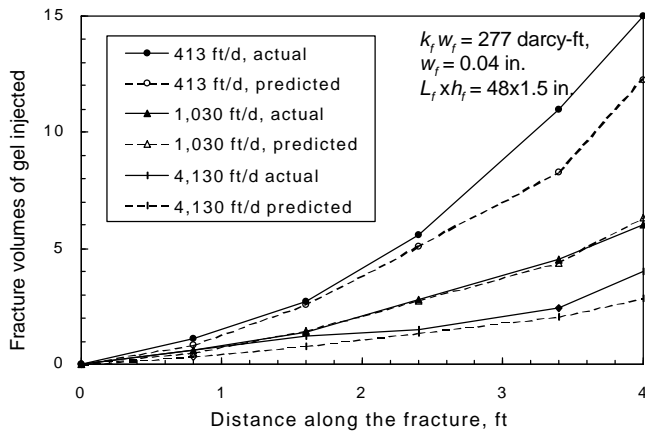


Fig. 8—Gel propagation in 48x1.5x0.04-in. fractures. Model 2: $u_l = 0.05 t^{-0.55}$.

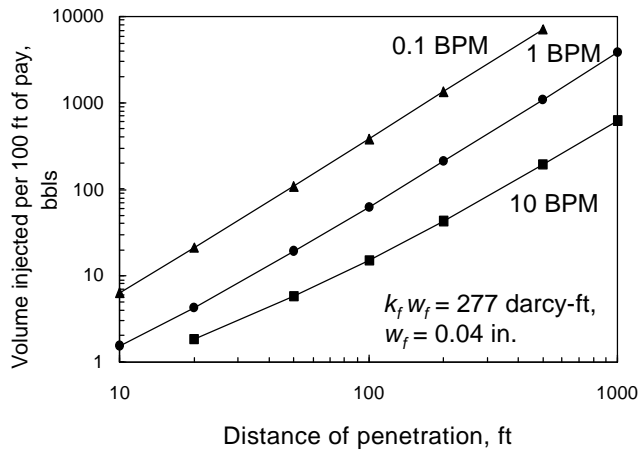


Fig. 9—Model 2 predictions in long two-wing fractures.

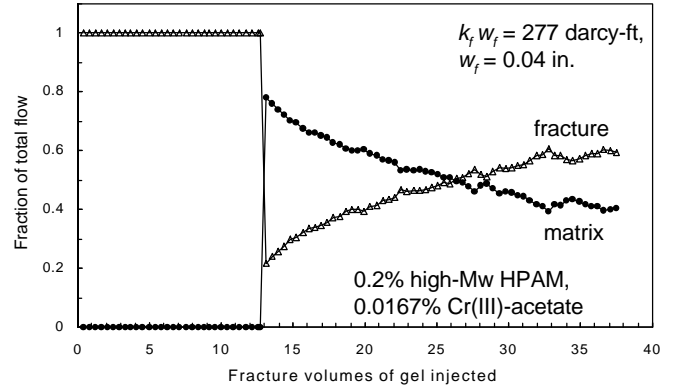


Fig. 10—Fraction of total flow measured at the core outlet (gel prepared with high-Mw HPAM).

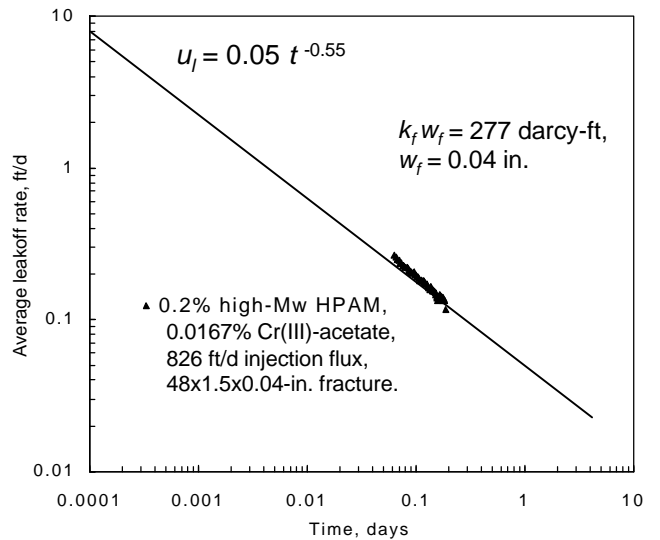


Fig. 11—Average leakoff rates using gel with high-Mw HPAM.